

Cooling Nanorotors by Elliptic Coherent Scattering

Jonas Schäfer,¹ Henning Rudolph,¹ Klaus Hornberger,¹ and Benjamin A. Stickler^{1,2}

¹*Faculty of Physics, University of Duisburg-Essen, Lotharstraße 1, 47048 Duisburg, Germany*

²*QOLS, Blackett Laboratory, Imperial College London, London SW7 2AZ, United Kingdom*



(Received 12 November 2020; accepted 29 March 2021; published 23 April 2021)

Simultaneously cooling the rotational and translational motion of nanoscale dielectrics into the quantum regime is an open task of great importance for sensing applications and quantum superposition tests. Here, we show that the six-dimensional ground state can be reached by coherent-scattering cooling with an elliptically polarized and shaped optical tweezer. We determine the cooling rates and steady-state occupations in a realistic setup and discuss applications for mechanical sensing and fundamental experiments.

DOI: 10.1103/PhysRevLett.126.163603

Introduction.—Optically levitating nanoparticles in ultrahigh vacuum yields an unprecedented degree of environmental isolation [1], rendering these systems ideally suited for precision sensing [2–5] and for mesoscopic quantum superposition tests [6–13]. For several applications it is crucial to cool the rotational and translational particle dynamics into the quantum regime. Recently, center-of-mass ground-state cooling has been achieved [14] using the method of coherent-scattering cooling [15,16]. In this Letter, we show that elliptically polarized and shaped tweezers enable cooling of nanoparticles into their simultaneous rotational and translational ground state.

The setup of coherent-scattering cooling consists of an optical tweezer levitating a nanoparticle inside a high-finesse cavity. If the tweezer is slightly red detuned from the cavity resonance, the particle motion loses energy by scattering tweezer photons into the cavity mode [17,18]. In contrast to conventional optomechanical setups [19–26], the cavity mode is nearly empty in the system’s steady state, leading to a significant reduction of laser phase noise [15] and holding the prospect of reaching the strong coupling regime [27].

What distinguishes levitated nanoparticles from other optomechanical systems is their ability to rotate. Desired or not, rotations of any levitated object must be controlled to fully exhaust its potential for sensing [28,29] and for future quantum superposition tests [7,9,10,30,31]. The classical rotation dynamics of nanoscale objects can be manipulated with linearly and circularly polarized lasers [32–36], enabling high-precision pressure [37] and torque [5] sensing. In the quantum regime, the nonharmonicity of the rotational spectrum gives rise to pronounced interference effects [11,38] and might be useful for quantum information processing [39,40].

Recent experiments demonstrate rotational cooling [41,42] by aligning particles in a space-fixed direction and damping their librations around this axis. While such

schemes allow reaching the quantum regime with ultrathin rod-shaped objects [25,43], they cease to be efficient once the particle shape significantly deviates from this idealization and rotational precession [44] becomes important. Specifically, rotations around the axis of maximal susceptibility experience only weak cooling but strongly influence the libration dynamics [42]. Finding a strategy to cool an arbitrarily shaped particle through the nonharmonic regime of rotations is therefore a prerequisite for future quantum applications of levitated objects.

In the present Letter and the accompanying article [45], we demonstrate how the nonlinearity of rotation dynamics can be overcome by coherent-scattering cooling with an elliptically polarized and shaped tweezer; see Fig. 1.

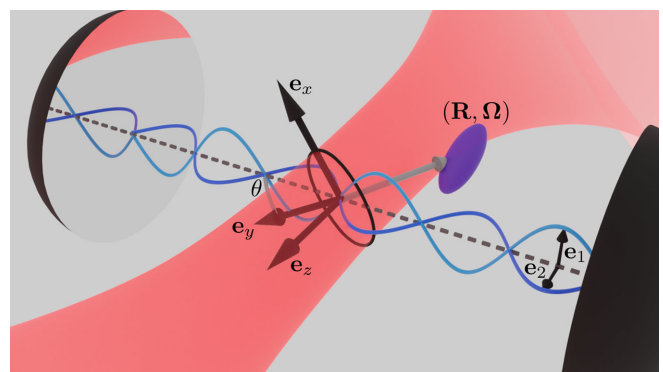


FIG. 1. An aspherical nanoparticle (purple ellipsoid) is trapped by a tweezer (red) inside an optical cavity with the principal axis (dashed line) orthogonal to the tweezer propagation direction. The tweezer is elliptically polarized and exhibits an elliptic intensity profile. The induced polarization field depends on the particle center-of-mass position \mathbf{R} and orientation Ω , driving two cavity modes (blue lines) with orthogonal polarizations $\mathbf{e}_{1,2}$. The resulting coupled nanoparticle–cavity dynamics can cool the nanoparticle motion into the 6D rotranslational quantum ground state.

The elliptical polarization of the light field introduces two space-fixed axes to control the rotations [46], rather than a single polarization axis. When placed inside a cavity, the nanoparticle rotations couple to two orthogonally polarized cavity modes, which in turn cool different mechanical degrees of freedom. For suitably chosen optical parameters, the resulting coupling cools subwavelength aspherical objects into their joint 6D rotranslational quantum ground state if they are close to spherical. We calculate the cooling rates and steady-state occupations for experimentally realistic situations, show that the expected torque sensitivities surpass state-of-the-art estimates by several orders of magnitude, and discuss how this setup can be used to generate ultrafast spinning, ultracold nanoparticles.

Nanoparticle–light interaction.—We consider an ellipsoidal particle of mass m , with three different principal-axis diameters $\ell_a < \ell_b < \ell_c$ and associated moments of inertia $I_a > I_b > I_c$. For subwavelength particles, the internal field is described by a linear susceptibility tensor $\chi(\Omega) = R(\Omega)\chi_0 R^T(\Omega)$ (Rayleigh-Gans approximation), where $R(\Omega)$ rotates from the space-fixed frame to the principal-axes frame and $\Omega = (\alpha, \beta, \gamma)$ denotes the Euler angles in the z - y' - z'' convention. The susceptibility tensor $\chi_0 = \text{diag}(\chi_a, \chi_b, \chi_c)$ contains the susceptibilities along the ellipsoid's principal axes. They can be calculated in terms of elliptic integrals [45,47], yielding $\chi_a < \chi_b < \chi_c$.

For a given laser field $\mathbf{E}(\mathbf{r})e^{-i\omega t}$, the time-averaged force and torque acting on the particle are dominated by the conservative optical potential

$$V_{\text{opt}}(\mathbf{R}, \Omega) = -\frac{\epsilon_0 V}{4} \mathbf{E}^*(\mathbf{R}) \cdot \chi(\Omega) \mathbf{E}(\mathbf{R}), \quad (1)$$

to first order of the particle volume V [25], with the center-of-mass position $\mathbf{R} = (x, y, z)$. Thus, if the electric field is linearly polarized, the optical potential tends to align the particle axis of maximal susceptibility with the field polarization.

In addition to the conservative potential (1), the laser also exerts a radiation pressure force and torque. The latter follow from the electric-field integral equation as [45]

$$\mathbf{F}_{\text{rad}} = \frac{\epsilon_0 k^3 V^2}{12\pi} \text{Im}[(\chi^2 \mathbf{E}^*) \cdot [\nabla \otimes (\chi \mathbf{E})]^T], \quad (2)$$

and

$$\mathbf{N}_{\text{rad}} = \frac{\epsilon_0 k^3 V^2}{12\pi} \text{Im}[(\chi^2 \mathbf{E}^*) \times \mathbf{E} - (\chi \mathbf{E}^*) \times (\chi \mathbf{E})], \quad (3)$$

where we omitted the dependence on \mathbf{R} and Ω . Force and torque are proportional to the cubed wave number k and to the squared particle volume, and are consistent with Ref. [25] for symmetric objects. An optical torque consistent with (3) has been experimentally observed to

accelerate nanorotors up to GHz frequencies [33–35,37]; it vanishes for linear field polarization.

Coupled nanoparticle–cavity dynamics.—If the particle is trapped inside a high-finesse optical cavity, the mechanical motion can couple strongly to two near-degenerate cavity modes; see Fig. 1. This interaction is determined by the total field,

$$\mathbf{E}(\mathbf{r}) = \sqrt{\frac{2\hbar\omega}{\epsilon_0 V_c}} \left[\epsilon \mathbf{e}_t f_t(\mathbf{r}) + \sum_{j=1,2} b_j \mathbf{e}_j f_c(\mathbf{r}) \right], \quad (4)$$

where ω denotes the tweezer frequency, V_c is the cavity mode volume, ϵ and $b_{1,2}$ are the dimensionless tweezer and cavity amplitudes, \mathbf{e}_t and $\mathbf{e}_{1,2}$ the corresponding polarization vectors, and $f_t(\mathbf{r})$ and $f_c(\mathbf{r})$ the mode functions.

The cavity resonance frequency ω_c is detuned from the tweezer frequency by $\Delta = \omega - \omega_c$. Near the cavity axis, the mode function can be approximated as a standing wave $f_c(\mathbf{r}) = \cos[k(\mathbf{e}_2 \times \mathbf{e}_1) \cdot \mathbf{r} + \phi]$, where ϕ describes the relative positioning of cavity and tweezer. The Gaussian envelope of the cavity modes with cavity waist w_c and length L determines the mode volume V_c , but can be neglected for the dynamics.

The tweezer quadrature ϵ is determined by the tweezer power and will be chosen real and positive. The tweezer mode function can be approximated by a traversing Gaussian beam with an elliptic intensity profile, $f_t(\mathbf{r}) = \exp[-(x^2/w_x^2 + y^2/w_y^2)/r^2(z)] e^{i[kz - \phi_t(\mathbf{r})]}/r(z)$ with the beam waists $w_{x,y}$. The latter determine the Rayleigh range z_R , which in turn sets the broadening factor $r(z)$ and the Gouy phase $\phi_t(\mathbf{r})$ [18,45].

We assume the tweezer propagation direction \mathbf{e}_z to be orthogonal to the cavity axis, with θ the angle between the latter and the y axis; see Fig. 1. The cavity mode polarizations can be chosen as $\mathbf{e}_1 = \cos\theta \mathbf{e}_x - \sin\theta \mathbf{e}_y$ and $\mathbf{e}_2 = \mathbf{e}_z$. To achieve trapping in all three orientational degrees of freedom, we choose the tweezer to be elliptically polarized, $\mathbf{e}_t = \cos\psi \mathbf{e}_{t,1} + i \sin\psi \mathbf{e}_{t,2}$, with the ellipticity $\psi \in [0, \pi/4]$. The two polarization axes are rotated with respect to the tweezer main axes by the angle ζ , $\mathbf{e}_{t,1} = \cos\zeta \mathbf{e}_x - \sin\zeta \mathbf{e}_y$ and $\mathbf{e}_{t,2} = \sin\zeta \mathbf{e}_x + \cos\zeta \mathbf{e}_y$.

The nanoparticle equations of motion are given by the optical potential (1) together with the nonconservative force (2) and torque (3). Taking the finite cavity line width κ into account, the dynamics of the cavity modes $b = (b_1, b_2)$ are described by $\dot{b} = (i\Delta_{\text{eff}} - \kappa_{\text{eff}})b + \eta$, with the vector $[\eta]_j = -\epsilon \mathbf{e}_j \cdot (iU_0 \chi + \gamma_{\text{sc}} \chi^2/2) \mathbf{e}_t f_c f_t$, the coupling frequency $U_0 = -\omega V/2V_c$, and the Rayleigh scattering rate $\gamma_{\text{sc}} = \omega k^3 V^2/6\pi V_c$. The matrices Δ_{eff} and κ_{eff} describe the effective detuning and linewidth for a given particle position and orientation,

$$[\Delta_{\text{eff}}]_{jj'} = \Delta \delta_{jj'} - U_0 f_c^2 \mathbf{e}_j \cdot \chi \mathbf{e}_{j'}, \quad (5)$$

and

$$[\kappa_{\text{eff}}]_{jj'} = \kappa \delta_{jj'} + \frac{\gamma_{\text{sc}}}{2} f_c^2 \mathbf{e}_j \cdot \chi^2 \mathbf{e}_{j'}. \quad (6)$$

It can be demonstrated that the combined rotational and translational particle motion is always cooled down if the tweezer is sufficiently far red detuned, i.e., for $\Delta < U_0 \chi_c$ [45]. In this limit, the potential is always stiffer when the particle moves up the potential slope than when it moves toward the minimum.

Deep trapping regime.—We harmonically expand the nanoparticle–cavity dynamics around the tweezer potential minimum $q_{\text{tw}} = (\mathbf{R}_{\text{tw}}, \Omega_{\text{tw}})$, where the axis with the largest (intermediate) susceptibility aligns in parallel to the stronger (weaker) tweezer polarization axis $\text{Re}(\mathbf{e}_r)$ [$\text{Im}(\mathbf{e}_r)$] [46]. At the minimum $\mathbf{R}_{\text{tw}} = (0, 0, 0)$ and $\Omega_{\text{tw}} = (-\zeta, \pi/2, 0)$ the cavity modes attain the amplitudes b_{tw} , implying that the effective detuning matrix (5) is diagonal and that mode b_2 is empty [45].

The coupling to the cavity modes as well as the nonconservative tweezer torque displace the equilibrium configuration $(q_{\text{eq}}, b_{\text{eq}})$ slightly away from the tweezer minimum $(q_{\text{tw}}, b_{\text{tw}})$. For small offsets, this does not affect the dynamics of the small deviations $\delta b = b - b_{\text{eq}}$ and of the small mechanical displacements described by the mode operators $a_q = (q - q_{\text{eq}} + ip_q/m_q \omega_q)/2q_{\text{zp}}$. Here, the zero-point amplitude $q_{\text{zp}} = \sqrt{\hbar/2m_q \omega_q}$ is determined by the Hamiltonian H_0 of the free translational and rotational motion [45], in terms of the effective masses $m_q^{-1} = \partial_{p_q}^2 H_0(q_{\text{tw}})$ and by the trapping frequencies $\omega_q^2 = \partial_q^2 V_{\text{opt}}(q_{\text{tw}}, b_{\text{tw}})/m_q$. The optomechanical coupling frequencies follow from the interaction potential (1) as $g_{jq} = -q_{\text{zp}} \partial_{b_j} \partial_q V_{\text{opt}}(q_{\text{tw}}, b_{\text{tw}})/\hbar$. These couplings imply that the optical mode δb_1 interacts only with coordinates that shift the effective detuning (5) along the \mathbf{e}_1 axis; i.e., $q \in S_1 = \{x, y, z, \alpha\}$. In a similar fashion, mode δb_2 couples only to $q \in S_2 = \{\beta, \gamma\}$. The equilibrium orientations of S_2 coincide with their minimal values in the tweezer potential because b_2 vanishes in the steady state.

The resulting total Hamiltonian decomposes into two noninteracting contributions, $H = H_1 + H_2$, with

$$\begin{aligned} \frac{H_j}{\hbar} = & \sum_{q \in S_j} \omega_q a_q^\dagger a_q - \sum_{qq' \in S_j} g_{qq'} (a_q + a_q^\dagger)(a_{q'} + a_{q'}^\dagger) \\ & - \sum_{q \in S_j} [g_{jq} \delta b_j (a_q + a_q^\dagger) + \text{H.c.}] - \Delta_j \delta b_j^\dagger \delta b_j. \end{aligned} \quad (7)$$

Here, the detunings $\Delta_j = [\Delta_{\text{eff}}(q_{\text{tw}})]_{jj}$ follow from (5) and the cavity-mediated mechanical coupling rates are $g_{qq'} = -q_{\text{zp}} q'_{\text{zp}} \partial_q \partial_{q'} V_{\text{opt}}(q_{\text{tw}}, b_{\text{tw}})/\hbar$.

Recoil heating.—So far, we discussed the conservative interaction between the mechanical degrees of freedom and the cavity modes. Recoil heating by incoherently scattered

tweezer photons and collisional heating by residual gas atoms limits the cooling process. For recoil heating, the resulting diffusion rates can be calculated either in a semiclassical picture [43] or from the Lindbladians of the exact quantum master equation [48]. For the center-of-mass modes $q \in \{x, y, z\}$, this yields the phonon heating rates [45]

$$\begin{aligned} \xi_q^{\text{rec}} = & \frac{\gamma_{\text{sc}} \epsilon^2}{5} k^2 q_{\text{zp}}^2 [(\chi_c^2 \cos^2 \psi + \chi_b^2 \sin^2 \psi)(2 + u \delta_{zq}) \\ & - \chi_c^2 \cos^2 \psi \delta_{xq} - \chi_b^2 \sin^2 \psi \delta_{yq}], \end{aligned} \quad (8)$$

with $u = 5(1 - 1/kz_R)^2$. A similar calculation for the librational degrees of freedom $q \in \{\alpha, \beta, \gamma\}$ yields the diffusion rates

$$\xi_q^{\text{rec}} = \gamma_{\text{sc}} \epsilon^2 q_{\text{zp}}^2 \Delta \chi_q^2 [1 - \sin^2 \psi \delta_{\beta q} - \cos^2 \psi \delta_{\gamma q}], \quad (9)$$

where $\Delta \chi_\alpha = |\chi_b - \chi_c|$, and cyclic permutations.

The corresponding diffusion rates due to collisions with residual gas atoms are $\xi_q^{\text{gas}} = k_B \gamma_q^{\text{gas}} T_g / \hbar \omega_q$, where T_g is the gas temperature and γ_q^{gas} denotes the gas damping constant [49]. We neglect heating due to tweezer phase noise, which can be diminished by destructive interference between the stationary intracavity field b_0 and a phase-locked pump field. The total heating rates are thus given by $\xi_q = \xi_q^{\text{rec}} + \xi_q^{\text{gas}}$.

Ground-state cooling.—The cavity-mediated coupling between the mechanical degrees of freedom leads to the appearance of hybrid mechanical modes $S'_1 = \{x', y', z', \alpha'\}$ and $S'_2 = \{\beta', \gamma'\}$, which can be determined by diagonalizing the first line of Eq. (7). However, because the cavity population is much smaller than the tweezer amplitude, $|b_j| \ll \epsilon$, the couplings fulfill $|g_{qq'}|^2 \ll \omega_q \omega_{q'}$ for most ellipticities, so that the hybridized modes S'_j are well approximated by the original modes S_j [50].

After transforming to the hybrid modes, each mechanical degree of freedom $Q \in S'_j$ with trapping frequencies ω_Q linearly interacts with the respective light mode b_j as quantified by the coupling constant g_Q . In the weak coupling approximation [51], the resulting cooling and heating rates due to enhanced anti-Stokes and Stokes scattering (Purcell effect) follow from a standard calculation as $\gamma_Q^\mp = 2|g_Q|^2 \kappa / [\kappa^2 + (\Delta_j \pm \omega_Q)^2]$. These expressions are valid for $\gamma_Q^\mp \ll \kappa$ and $\gamma_Q^\mp \gamma_{Q'}^\mp \ll (\omega_Q - \omega_{Q'})^2$, where $Q, Q' \in S'_j$. From this, one obtains the stationary mechanical mode occupations $n_Q = (\gamma_Q^+ + \xi_Q) / (\gamma_Q^- - \gamma_Q^+)$.

The resulting weak coupling steady-state occupations for three ellipsoidally shaped particles are listed in Table I. The corresponding cavity parameters and nanoparticle specifications are close to state-of-the-art experiments [14]. Based on this we conclude that the 6D quantum ground state is realistically achievable by elliptic coherent-scattering cooling. Even though the rotation of an exactly spherical

TABLE I. Stationary phonon occupations for three silicon ellipsoids with principal axes (ℓ_a, ℓ_b, ℓ_c) in the weak-coupling approximation. Room temperature (r.t.) indicates that the respective degree of freedom is not cooled in the deep trapping regime. The occupations are obtained for a 1550 nm cavity, at ellipticity angle $\psi = \pi/6$, $\zeta = 0$, and 10^{-9} mbar. All other parameters were chosen to achieve efficient cooling. (70, 70, 70): cavity length $L = 3$ mm, cavity waist $w_c = 40$ μm , linewidth $\kappa = 300$ kHz, tweezer power $P = 0.5$ W, waists $w_x = 1.6$ μm , $w_y = 1.3$ μm , detuning $\Delta = -500$ kHz, $\theta = \pi/4$, and $\phi = 3\pi/8$. (25, 40, 100), first row: same as for (70, 70, 70), except $P = 0.1$ W, $\kappa = 2$ MHz, $\Delta = -11$ MHz, $\theta = \pi/2$, and $\phi = 0$. (25, 40, 100), second row: same as for (70, 70, 70). (69, 70, 71): $L = 1.5$ mm, $w_c = 30$ μm , $\kappa = 600$ kHz, $P = 0.1$ W, $w_x = 800$ nm, $w_y = 650$ nm, $\Delta = -1.8$ MHz, $\theta = \pi/4$, and $\phi = 3\pi/8$. The steady-state occupations for the x' and y' modes are approximate because they are not in the strict weak-coupling regime for the given parameters.

Particle shape (ℓ_a, ℓ_b, ℓ_c) (nm)	Cooled by b_1				Cooled by b_2	
	$n_{x'}$	$n_{y'}$	$n_{z'}$	n_d	n_β	n_γ
(70,70,70)	0.1	0.1	0.5	r.t.	r.t.	r.t.
(25,40,100)	r.t.	r.t.	$\gtrsim 10^2$	0.1	0.2	0.1
	0.2	0.3	0.4	$\gtrsim 10^3$	$\gtrsim 10^3$	$\gtrsim 10^3$
(69,70,71)	0.1	0.1	0.9	0.3	0.9	0.2

particle (first row) cannot be cooled, the orientation can be driven into the quantum ground state in the other cases considered. For increasingly anisotropic particles (second and third row) the librational and translational frequencies diverge, rendering simultaneous cooling inefficient. Nonetheless, appropriately choosing the detuning allows one to efficiently cool either the rotations or the center-of-mass motion to the ground state. For slightly aspherical particles (fourth row), all six degrees of freedom can be simultaneously cooled into their quantum ground state. This regime can be reached in particular if all trapping frequencies lie within the cavity linewidth while being

sufficiently separated to avoid dark modes. The impact of the particle anisotropy is discussed in Ref. [45]. In Table I, gas scattering is relevant only for the β' and γ' degrees of freedom in the fourth row. The corresponding damping constants are $\gamma_q^{\text{gas}} \approx 5p_g \ell_b^2 \sqrt{2\pi\mu}/6m \sqrt{k_B T_g}$ [49] with $T_g = 300$ K and the mass of helium μ .

The cooling timescales $\log(k_B T_0 / \hbar \omega_Q n_Q) / (\gamma_Q^- - \gamma_Q^+)$ are on the order of a few hundred microseconds for the translation and in the two-digit millisecond regime for the librations, assuming a starting temperature of $T_0 = 40$ K (librational trapping). Nonharmonicities in H_0 give rise to higher harmonics in the cavity output fields as long as the phonon number exceeds a few hundred. This is illustrated in Fig. 2, which shows the power spectral densities of the two cavity output modes for three different gas pressures [45]. Figure 2(c) presents the steady-state occupations as a function of tweezer ellipticity ψ , demonstrating that ground-state cooling is impossible for linear ($\psi = 0$) and circular ($\psi = \pi/4$) polarization, and that the optimal cooling regime is close to $\psi = \pi/6$. Orientational trapping becomes unstable when approaching circular polarization because the time-averaged potential can no longer confine the rotation in the polarization plane.

Discussion.—Coherent-scattering cooling with an elliptically polarized tweezer offers an attractive setup for efficiently cooling nanoparticles into the quantum regime in all their rotranslational degrees of freedom. This has great potential for sensing applications and for fundamental quantum experiments, even with spherical objects, because exact sphericity can never be guaranteed.

Specifically, torque sensing can be best performed by monitoring the mode b_2 , which is unaffected by the center-of-mass motion. The minimally detectable torque from measuring the two librational degrees of freedom β, γ is $N_2^{\text{min}} / \sqrt{B} \approx \sqrt{4\hbar\omega_\gamma I_c \xi_{\gamma'}} \approx 3.9 \times 10^{-30} \text{ Nm} / \sqrt{\text{Hz}}$, where B is the measurement bandwidth [52]. This would improve current experiments by orders of magnitude [5] and enable

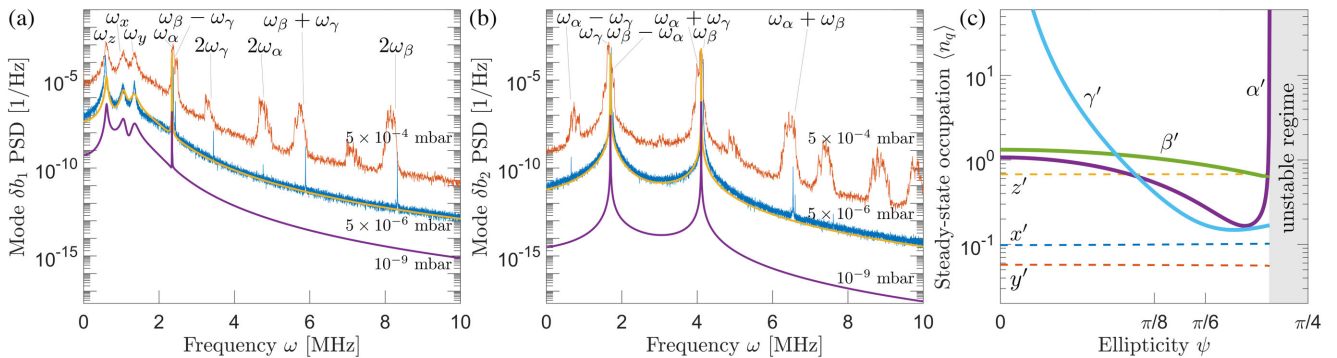


FIG. 2. Analytic (thick solid line) and numerical (thin solid line) steady-state power spectral densities (PSDs) of the cavity modes δb_1 (a) and δb_2 (b). The PSDs are displayed for the three different gas pressures $p_g = 5 \times 10^{-4}$ mbar, $p_g = 5 \times 10^{-6}$ mbar, and $p_g = 10^{-9}$ mbar (from top to bottom). The additional peaks found numerically at high pressures are higher harmonics of the ground modes generated by the nonlinearity of nanoparticle rotations. All other parameters are chosen as for (69, 70, 71) nm in Table I. (c) Steady-state occupations as a function of the tweezer ellipticity ψ for the (69, 70, 71) nm particle in Table I.

the observation of rotational quantum friction [53] and the Casimir torque [54]. Simultaneously monitoring both cavity output modes also opens the door to combined force and torque measurements using different degrees of freedom of a single levitated object.

Even for particle shapes where 6D cooling is inefficient, elliptic coherent scattering can prepare their orientational degrees of freedom in the quantum regime. This setup is therefore ideally suited for preparing rotational quantum superposition tests with nanoscale rotors [11,38]. For instance, cooling an asymmetric rotor into its quantum ground state and then far detuning and circularly polarizing the tweezer, so that the particle is angularly accelerated by the nonconservative torque (3), generates a cold but rapidly rotating state as required to observe quantum persistent tennis racket flips [38] and acousto-rotational coupling [55]. For the aspherical particles considered Table I, GHz rotation frequencies can be readily achieved by switching to circular polarization and detuning the tweezer from the cavity resonance. For instance, the (25, 40, 100) nm particle (Table I), initially prepared in the steady state and then rotationally accelerated by the nonconservative torque (3), reaches the quantum tennis racket regime [38] in a matter of milliseconds; see Fig. 3.

Finally, the isolated librational S'_2 modes are ideally suited for trapped quantum experiments [12,13,56] because they are weakly affected by Rayleigh scattering of tweezer

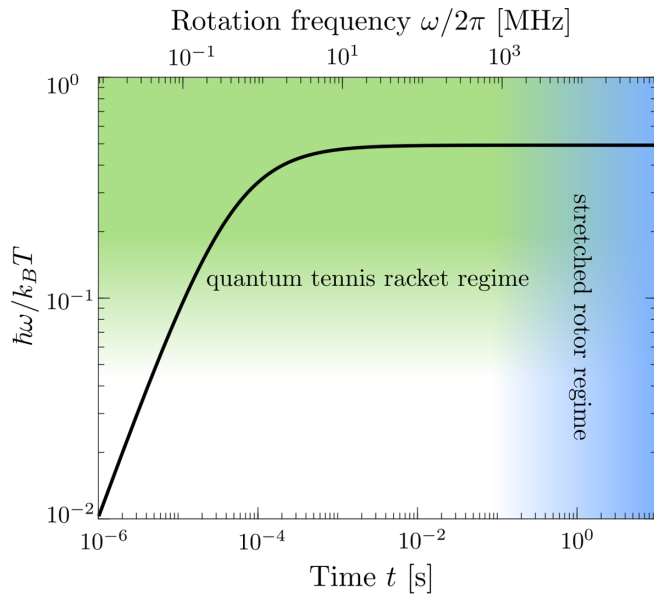


FIG. 3. Rotationally cold nanoparticles can be propelled into the regimes where quantum tennis racket flips [38] and the effects of centrifugal stretching [55] are observable. The tennis racket regime is reached for $\hbar\omega/k_B T \gtrsim 0.1$, where the rotational temperature T characterizes the angular momentum width. Centrifugal stretching of the particle starts playing a role once the nanoparticle endpoint velocities become comparable to the speed of sound divided by its dielectric permittivity.

photons (9), leading to coherence times larger than those of the other mechanical modes by about one order of magnitude. For instance, the expected γ' coherence time is on the order of 0.6–1.1 ms for the 6D ground state setup in Table I.

In summary, coherent-scattering cooling with an elliptically polarized tweezer enables simultaneous rotranslational ground-state cooling of nanoscale dielectrics. This setup may well serve as a building block for future quantum experiments and sensors with levitated nanoparticles.

We thank Stephan Troyer for helpful discussions and Issam Bouchdad for assistance in creating Fig. 1. K. H. acknowledges funding from the Deutsche Forschungsgemeinschaft (DFG, German Research Foundation), Grant No. 394398290; B. A. S. acknowledges funding from the European Unions Horizon 2020 research and innovation program under Marie Skłodowska-Curie Grant Agreement No. 841040 and from the Deutsche Forschungsgemeinschaft (DFG, German Research Foundation), Grant No. 439339706.

J. S. and H. R. contributed equally to this work.

- [1] J. Millen, T. S. Monteiro, R. Pettit, and A. N. Vamivakas, Optomechanics with levitated particles, *Rep. Prog. Phys.* **83**, 026401 (2020).
- [2] J. Chaste, A. Eichler, J. Moser, G. Ceballos, R. Rurali, and A. Bachtold, A nanomechanical mass sensor with yoctogram resolution, *Nat. Nanotechnol.* **7**, 301 (2012).
- [3] G. Ranjit, M. Cunningham, K. Casey, and A. A. Geraci, Zeptonewton force sensing with nanospheres in an optical lattice, *Phys. Rev. A* **93**, 053801 (2016).
- [4] D. Hempston, J. Vovrosh, M. Toroš, G. Winstone, M. Rashid, and H. Ulbricht, Force sensing with an optically levitated charged nanoparticle, *Appl. Phys. Lett.* **111**, 133111 (2017).
- [5] J. Ahn, Z. Xu, J. Bang, P. Ju, X. Gao, and T. Li, Ultra-sensitive torque detection with an optically levitated nanorotor, *Nat. Nanotechnol.* **15**, 89 (2020).
- [6] O. Romero-Isart, A. C. Pflanzer, F. Blaser, R. Kaltenbaek, N. Kiesel, M. Aspelmeyer, and J. I. Cirac, Large Quantum Superpositions and Interference of Massive Nanometer-Sized Objects, *Phys. Rev. Lett.* **107**, 020405 (2011).
- [7] J. Bateman, S. Nimmrichter, K. Hornberger, and H. Ulbricht, Near-field interferometry of a free-falling nanoparticle from a point-like source, *Nat. Commun.* **5**, 4788 (2014).
- [8] M. Arndt and K. Hornberger, Testing the limits of quantum mechanical superpositions, *Nat. Phys.* **10**, 271 (2014).
- [9] C. Wan, M. Scala, G. Morley, A. A. Rahman, H. Ulbricht, J. Bateman, P. Barker, S. Bose, and M. Kim, Free Nano-object Ramsey Interferometry for Large Quantum Superpositions, *Phys. Rev. Lett.* **117**, 143003 (2016).
- [10] R. Kaltenbaek, M. Aspelmeyer, P. F. Barker, A. Bassi, J. Bateman, K. Bongs, S. Bose, C. Braxmaier, Č. Brukner, B. Christophe *et al.*, Macroscopic quantum resonators

- (MAQRO): 2015 update, *Eur. Phys. J. Quantum Technol.* **3**, 5 (2016).
- [11] B. A. Stickler, B. Papendell, S. Kuhn, B. Schirnski, J. Millen, M. Arndt, and K. Hornberger, Probing macroscopic quantum superpositions with nanorotors, *New J. Phys.* **20**, 122001 (2018).
- [12] H. Rudolph, K. Hornberger, and B. A. Stickler, Entangling levitated nanoparticles by coherent scattering, *Phys. Rev. A* **101**, 011804 (2020).
- [13] A. A. Rakhubovsky, D. W. Moore, U. Delić, N. Kiesel, M. Aspelmeyer, and R. Filip, Detecting nonclassical correlations in levitated cavity optomechanics, *Phys. Rev. Applied* **14**, 054052 (2020).
- [14] U. Delić, M. Reisenbauer, K. Dare, D. Grass, V. Vuletić, N. Kiesel, and M. Aspelmeyer, Cooling of a levitated nanoparticle to the motional quantum ground state, *Science* **367**, 892 (2020).
- [15] U. Delić, M. Reisenbauer, D. Grass, N. Kiesel, V. Vuletić, and M. Aspelmeyer, Cavity Cooling of a Levitated Nanosphere by Coherent Scattering, *Phys. Rev. Lett.* **122**, 123602 (2019).
- [16] D. Windey, C. Gonzalez-Ballester, P. Maurer, L. Novotny, O. Romero-Isart, and R. Reimann, Cavity-Based 3D Cooling of a Levitated Nanoparticle via Coherent Scattering, *Phys. Rev. Lett.* **122**, 123601 (2019).
- [17] T. Salzburger and H. Ritsch, Collective transverse cavity cooling of a dense molecular beam, *New J. Phys.* **11**, 055025 (2009).
- [18] C. Gonzalez-Ballester, P. Maurer, D. Windey, L. Novotny, R. Reimann, and O. Romero-Isart, Theory for cavity cooling of levitated nanoparticles via coherent scattering: master equation approach, *Phys. Rev. A* **100**, 013805 (2019).
- [19] D. E. Chang, C. Regal, S. Papp, D. Wilson, J. Ye, O. Painter, H. J. Kimble, and P. Zoller, Cavity opto-mechanics using an optically levitated nanosphere, *Proc. Natl. Acad. Sci. U.S.A.* **107**, 1005 (2010).
- [20] O. Romero-Isart, M. L. Juan, R. Quidant, and J. I. Cirac, Toward quantum superposition of living organisms, *New J. Phys.* **12**, 033015 (2010).
- [21] P. Barker and M. Schneider, Cavity cooling of an optically trapped nanoparticle, *Phys. Rev. A* **81**, 023826 (2010).
- [22] P. Asenbaum, S. Kuhn, S. Nimmrichter, U. Sezer, and M. Arndt, Cavity cooling of free silicon nanoparticles in high vacuum, *Nat. Commun.* **4**, 2743 (2013).
- [23] N. Kiesel, F. Blaser, U. Delić, D. Grass, R. Kaltenbaek, and M. Aspelmeyer, Cavity cooling of an optically levitated submicron particle, *Proc. Natl. Acad. Sci. U.S.A.* **110**, 14180 (2013).
- [24] J. Millen, P. Fonseca, T. Mavrogordatos, T. Monteiro, and P. Barker, Cavity Cooling a Single Charged Levitated Nanosphere, *Phys. Rev. Lett.* **114**, 123602 (2015).
- [25] B. A. Stickler, S. Nimmrichter, L. Martinetz, S. Kuhn, M. Arndt, and K. Hornberger, Rotational cavity cooling of dielectric rods and disks, *Phys. Rev. A* **94**, 033818 (2016).
- [26] P. Fonseca, E. Aranas, J. Millen, T. Monteiro, and P. Barker, Nonlinear Dynamics and Strong Cavity Cooling of Levitated Nanoparticles, *Phys. Rev. Lett.* **117**, 173602 (2016).
- [27] A. de los Ros Sommer, N. Meyer, and R. Quidant, Strong optomechanical coupling at room temperature by coherent scattering, *Nat. Commun.* **12**, 276 (2021).
- [28] D. C. Moore, A. D. Rider, and G. Gratta, Search for Millicharged Particles Using Optically Levitated Microspheres, *Phys. Rev. Lett.* **113**, 251801 (2014).
- [29] A. D. Rider, D. C. Moore, C. P. Blakemore, M. Louis, M. Lu, and G. Gratta, Search for Screened Interactions Associated with Dark Energy below the 100 μm Length Scale, *Phys. Rev. Lett.* **117**, 101101 (2016).
- [30] M. Scala, M. S. Kim, G. W. Morley, P. F. Barker, and S. Bose, Matter-Wave Interferometry of a Levitated Thermal Nano-oscillator Induced and Probed by a Spin, *Phys. Rev. Lett.* **111**, 180403 (2013).
- [31] C. Knobloch, B. A. Stickler, C. Brand, M. Sclafani, Y. Lilach, T. Juffmann, O. Cheshnovsky, K. Hornberger, and M. Arndt, On the role of the electric dipole moment in the diffraction of biomolecules at nanomechanical gratings, *Fortschr. Physik* **65**, 1600025 (2017).
- [32] T. M. Hoang, Y. Ma, J. Ahn, J. Bang, F. Robicheaux, Z.-Q. Yin, and T. Li, Torsional Optomechanics of a Levitated Nonspherical Nanoparticle, *Phys. Rev. Lett.* **117**, 123604 (2016).
- [33] S. Kuhn, A. Kosloff, B. A. Stickler, F. Patolsky, K. Hornberger, M. Arndt, and J. Millen, Full rotational control of levitated silicon nanorods, *Optica* **4**, 356 (2017).
- [34] J. Ahn, Z. Xu, J. Bang, Y.-H. Deng, T. M. Hoang, Q. Han, R.-M. Ma, and T. Li, Optically Levitated Nanodumbbell Torsion Balance and GHz Nanomechanical Rotor, *Phys. Rev. Lett.* **121**, 033603 (2018).
- [35] R. Reimann, M. Doderer, E. Hebestreit, R. Diehl, M. Frimmer, D. Windey, F. Tebbenjohanns, and L. Novotny, GHz Rotation of an Optically Trapped Nanoparticle in Vacuum, *Phys. Rev. Lett.* **121**, 033602 (2018).
- [36] F. van der Laan, R. Reimann, A. Militaru, F. Tebbenjohanns, D. Windey, M. Frimmer, and L. Novotny, Optically levitated rotor at its thermal limit of frequency stability, *Phys. Rev. A* **102**, 013505 (2020).
- [37] S. Kuhn, B. A. Stickler, A. Kosloff, F. Patolsky, K. Hornberger, M. Arndt, and J. Millen, Optically driven ultra-stable nanomechanical rotor, *Nat. Commun.* **8**, 1670 (2017).
- [38] Y. Ma, K. E. Khosla, B. A. Stickler, and M. S. Kim, Quantum Persistent Tennis Racket Dynamics of Nanorotors, *Phys. Rev. Lett.* **125**, 053604 (2020).
- [39] A. L. Grimsmo, J. Combes, and B. Q. Baragiola, Quantum Computing with Rotation-Symmetric Bosonic Codes, *Phys. Rev. X* **10**, 011058 (2020).
- [40] V. V. Albert, J. P. Covey, and J. Preskill, Robust Encoding of a Qubit in a Molecule, *Phys. Rev. X* **10**, 031050 (2020).
- [41] T. Delord, P. Huillery, L. Nicolas, and G. Hétet, Spin-cooling of the motion of a trapped diamond, *Nature* **580**, 56 (2020).
- [42] J. Bang, T. Seberon, P. Ju, J. Ahn, Z. Xu, X. Gao, F. Robicheaux, and T. Li, Five-Dimensional Cooling and Nonlinear Dynamics of an Optically Levitated Nanodumbbell, *Phys. Rev. Research* **2**, 043054 (2020).
- [43] T. Seberon and F. Robicheaux, Distribution of laser shot-noise energy delivered to a levitated nanoparticle, *Phys. Rev. A* **102**, 033505 (2020).
- [44] M. Rashid, M. Toroš, A. Setter, and H. Ulbricht, Precession Motion in Levitated Optomechanics, *Phys. Rev. Lett.* **121**, 253601 (2018).

- [45] H. Rudolph, J. Schäfer, B. A. Stickler, and K. Hornberger, companion paper, Theory of nanoparticle cooling by elliptic coherent scattering, *Phys. Rev. A* **103**, 043514 (2021).
- [46] H. Stapelfeldt and T. Seideman, Colloquium: Aligning molecules with strong laser pulses, *Rev. Mod. Phys.* **75**, 543 (2003).
- [47] H. van de Hulst, *Light Scattering by Small Particles* (Dover, New York, 1981).
- [48] B. A. Stickler, B. Papendell, and K. Hornberger, Spatio-orientational decoherence of nanoparticles, *Phys. Rev. A* **94**, 033828 (2016).
- [49] L. Martinetz, K. Hornberger, and B. A. Stickler, Gas-induced friction and diffusion of rigid rotors, *Phys. Rev. E* **97**, 052112 (2018).
- [50] M. Toroš and T. S. Monteiro, Quantum sensing and cooling in three-dimensional levitated cavity optomechanics, *Phys. Rev. Research* **2**, 023228 (2020).
- [51] I. Wilson-Rae, N. Nooshi, J. Dobrindt, T. J. Kippenberg, and W. Zwerger, Cavity-assisted backaction cooling of mechanical resonators, *New J. Phys.* **10**, 095007 (2008).
- [52] Z.-Q. Yin, A. A. Geraci, and T. Li, Optomechanics of levitated dielectric particles, *Int. J. Mod. Phys. B* **27**, 1330018 (2013).
- [53] R. Zhao, A. Manjavacas, F. J. G. de Abajo, and J. Pendry, Rotational Quantum Friction, *Phys. Rev. Lett.* **109**, 123604 (2012).
- [54] Z. Xu and T. Li, Detecting casimir torque with an optically levitated nanorod, *Phys. Rev. A* **96**, 033843 (2017).
- [55] D. Hümmer, R. Lampert, K. Kustura, P. Maurer, C. Gonzalez-Ballester, and O. Romero-Isart, Acoustic and optical properties of a fast-spinning dielectric nanoparticle, *Phys. Rev. B* **101**, 205416 (2020).
- [56] O. Romero-Isart, A. C. Pflanzer, M. L. Juan, R. Quidant, N. Kiesel, M. Aspelmeyer, and J. I. Cirac, Optically levitating dielectrics in the quantum regime: Theory and protocols, *Phys. Rev. A* **83**, 013803 (2011).